Chemical Engineering Journal 213 (2012) 135–141

Contents lists available at SciVerse ScienceDirect

Chemical Engineering Journal

journal homepage: www.elsevier.com/locate/cej

Removal of mercury from aqueous solutions by malt spent rootlets

Vasileios A. Anagnostopoulos [a], Ioannis D. Manariotis [b,*], Hrissi K. Karapanagioti [a], Constantinos V. Chrysikopoulos [b]

[a] Department of Chemistry, University of Patras, Patras 26500, Greece
[b] Department of Civil Engineering, Environmental Engineering Laboratory, University of Patras, Patras 26500, Greece

HIGHLIGHTS

- Malt spent rootlets (MSR) are promising biosorbents for mercury removal.
- Malt spent rootlets (MSR) exhibit satisfactory sorption capacity and fast kinetics.
- Film diffusion and intra-particle diffusion play an important role on mercury sorption.

ARTICLE INFO

Article history:
Received 26 April 2012
Received in revised form 7 September 2012
Accepted 16 September 2012
Available online 5 October 2012

Keywords:
Biosorbents
Heavy metals
Sorption
Desorption
Sorption kinetic models

ABSTRACT

Mercury poses a severe threat to environment due to its toxicity, even at low concentrations. Biosorption is a promising, low cost, and environmentally friendly clean up technique. Malt spent rootlets (MSR), a brewery by-product, were used as sorbents for the removal of mercury from aquatic systems. The effect of the solution pH, contact time between sorbent, solid to liquid ratio, and initial mercury concentration on mercury removal were investigated experimentally. It was found that the optimum pH for the mercury sorption onto MSR was approximately 5. Sorption kinetic experiments revealed that mercury sorption is a relatively rapid process, where film diffusion and intra-particle diffusion play an important role. The kinetic data were successfully described by both the pseudo-second-order and Elovich models. The isotherm data were adequately fitted by the Langmuir model determining a monolayer capacity q_{max} equal to 50 mg/g and suggesting a functional group-limited sorption process. MSR were capable of removing significant amounts of mercury, mainly due to the carboxyl and phosphonate groups of their surfaces. Mercury desorption from the MSR was found to be most effective with HCl 0.1 M.

1. Introduction

Mercury, even at low concentrations, is of particular concern due to its toxicity [1]. It is classified among priority hazardous compounds according to the European Union (EU) legislation [2,3]. The maximum allowable level for mercury in surface waters is 0.07 μg/L [3]. Mercury is released into the environment via natural processes (i.e. volcanic eruptions), anthropogenic activities (i.e. coal burning power plants), accidentally due to manufacture, breakage or disposal of products that contain mercury [4,5].

Removal of metal ions from aquatic systems has been practiced for decades, but commonly employed physico-chemical techniques, such as electrochemical treatment, ion exchange, reverse osmosis, precipitation, may exhibit serious drawbacks. For example, non-selective precipitation generates highly toxic metallic sludge; furthermore, ion exchange and reverse osmosis exhibit low efficiency at low concentrations and high operational cost [6]. However, biotechnological approaches, especially biosorption, may be more desirable due to lower cost and higher efficiency [6,7]. The term biosorption refers to the accumulation of metal ions by materials of biological origin, and consists of two steps: contact of the biomass with the metal contaminated wastewater, and separation of the metal-loaded biosorbent from the metal-depleted effluent [8]. Biomaterials have proven capability to take up heavy metals from aqueous solutions mainly due to carboxyl, hydroxyl, and phosphate active groups, which can bind metal ions [6]. The major advantages of biosorption are the low cost, high removal efficiency, biosorbent regeneration, and metal recovery [6].

In recent years, considerable research efforts by numerous investigators were focused on the removal of Hg(II) from water by sorption processes, and the evaluation of sorption capacity of various materials. Activated carbon [9,10] or polymer-coated activated carbon [11] have been shown to effectively absorb Hg(II); however, they are relatively expensive materials. Alternative biomaterials, such as fern, fruit derived biomass and leaves of castor

* Corresponding author.
E-mail address: idman@upatras.gr (I.D. Manariotis).

1385-8947/$ - see front matter © 2012 Elsevier B.V. All rights reserved.
http://dx.doi.org/10.1016/j.cej.2012.09.074

tree have also been investigated for mercury sorption with encouraging results [12–15]. Malt spent rootlets have not been used before for mercury removal.

The objective of the present work was to evaluate the potential use of malt spent rootlets (MSR), a low cost biosorbent, to remove Hg(II) from pure aqueous solutions by sorption. Batch experiments were conducted to obtain the optimum sorption conditions under different pH, biomass dose, and contact time. Furthermore, the effect of different leaching solutions on Hg(II) desorption from MSR was examined.

2. Materials and methods

2.1. Biomass

The MSR were obtained from the Athenian Brewery S.A. (Patras, Greece). The biomass was dried overnight at 50 °C, and sieved. The fraction of 0.150–1.180 mm was selected for the experiments.

The study of the MSR functional groups, was performed by Fourier Transform Infrared Analysis (FTIR) by the KBr disc method using a Perkin Elmer (model 16PC FT-IR) spectrophotometer. Scanning electron microscopy (SEM) was conducted on MSR after 2 and 24 h contact time with mercury using a scanning electron microscope (JEOL 6300, JEOL Ltd.).

The ability of MSR to swell was quantified through dry impregnation with distilled water. Various small amounts of dry MSR were weighted in porcelain crucibles. Using glass microsyringes (10 and 100 μL), small volumes of distilled water were continuously added and mixed with the MSR. The water added was absorbed by the swelling MSR. It was assumed that MSR was completely saturated when no more distilled water was absorbed and the MSR stopped swelling. The water volume needed to completely saturate a given mass of MSR was measured by a microsyringe.

2.2. Sorption experiments

A standard solution containing 50 mg/L Hg(II) was prepared by dissolving $HgCl_2$ (Merck) in distilled water. A small portion (10 mL) of the standard mercury solution was transferred into 15 mL polypropylene test tubes containing 10 mg of MSR. The tubes were hooked on a rotator (J.P. Selecta, Spain) for a specified time (5–5760 min). Subsequently, the tubes were placed vertically for the MSR to settle. The effect of pH on Hg(II) sorption onto MSR was examined at three different pH values (pH = 2, 3.5, and 5). The relatively narrow range of the selected pH values was dictated by the relatively low Hg(II) precipitation limit. For the isotherm experiments, different MSR masses and 10 mL solutions with different initial Hg(II) concentrations were brought in contact in 15 mL polypropylene test tubes for 24 h at pH = 5. All experiments were performed in duplicates.

2.3. Desorption experiments

Batch experiments were conducted to evaluate the desorption of Hg(II) from MSR. Four different desorption chemical solutions (NaCl, EDTA, HCl, and HNO_3) all at 0.1 M, and one blank solution (distilled water) were tested. These are the most frequently used agents for desorbing mercury from biomaterials [9,12,13]. Initially, 10 mL of the standard mercury solution were added into a vial containing 10 mg MSR. After 24 h of rotation, the residual Hg(II) concentration in the supernatant was determined. MSR was filtered and the biomass was washed three times with distilled water. Subsequently, 10 mL of each desorption solution were introduced and the system biomass-eluting agent was rotated for 24 h. Finally, the desorbed Hg(II) concentration in the aqueous phase was determined.

2.4. Analytical methods

The Hg(II) concentration was measured colorimetrically following the Michler's thioketone method [14]. An appropriate sample volume of the supernatant (200–1000 μL) was transferred into a 10 mL volumetric flask. Then, 1 mL buffer solution at pH 5.5 (9.4 g sodium acetate trihydrate dissolved in 50 mL of distilled water and 0.835 mL of acetic acid), and 5 mL of reagent solution (0.0020 g of 4,4-bis(dimethylamino)-thiobenzophenone (Michler's thioketone) in 50 mL of 1-propanol) were added. The flask was filled up to the 10 mL mark with a 30:70 (v/v) 1-propanol:distilled-water solution. The absorbance of the complex formed was measured at 565 nm with a UV–VIS spectrophotometer (U1100, Hitachi).

3. Results and discussion

3.1. Effect of pH

The results of the mercury uptake (q) for three different pH values are presented in Fig. 1. Clearly, the biosorption capacity is strongly affected by the initial pH of the aqueous Hg(II) solution. More specifically the biosorption capacity increases with increasing pH. Worthy to note is that at pH > 6, mercury precipitates [16]. The speciation of a solution containing 25 mg/L initial mercury concentration in distilled water, predicted by a commercial software (Hydra-Medusa Equilibrium Diagrams), is shown in Fig. 2.

Solution pH affects both the metal ion speciation and the ionization state of the MSR surface functional groups. At strong acidic conditions, surface functional groups are protonated, thus the approach of positively charged species is inhibited. As pH increases, the negative charge density on the MSR surface increases due to deprotonation of active sites, and therefore the approach of positively charged ions is promoted [17,18]. In this study, mercury species are neutral throughout the pH range tested (see Fig. 2). Consequently, the decrease of the MSR surface positive charge seems to be the main reason for the uptake increase. At low pH values (pH < 4.5), mercury exists mostly in the form of $HgCl_2$, and as the solution pH increases, the solubility of mercury decreases due to extensive hydrolysis (the percentage of HgClOH and $Hg(OH)_2$ species increases), hence the MSR sorption capacity increases to a certain limit depending on the mercury fraction remaining in solution. It has been reported in literature that hydroxyl-mercury species (such as HgClOH found at higher pH) are related to the increased mercury uptake, whereas chloride–mercury species (such

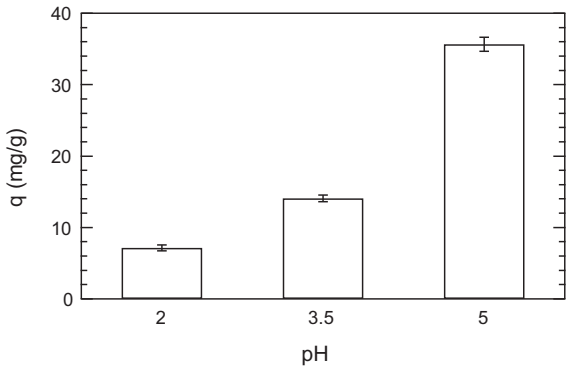

Fig. 1. Effect of solution pH on sorption capacity after 24 h mixing with C_o = 50 mg Hg(II)/L.

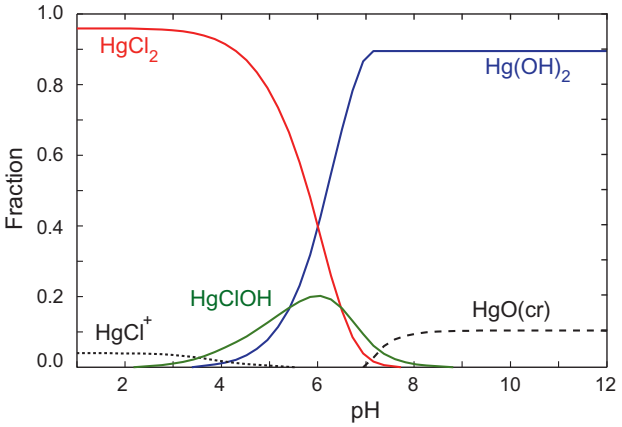

Fig. 2. Speciation of mercury in distilled water (C_o = 25 mg/L).

as $HgCl_2$ predominant at lower pH) are not preferentially sorbed [19,20]. Furthermore, the pH range of 5–6 is optimum for mercury sorption onto various sorbents such as rubber waste [19], chemically pre-treated coal [21], bark [16], bracken fern [15], fungal biomass [22] and microalgae [23]. Finally, it should be noted that MSR show a significant capacity to remove mercury even under strong acidic conditions, which could be significant for mercury recovery from strongly acidic aquatic systems like mining effluents [24].

3.2. Effect of solid/liquid ratio

The experimental data presented in Fig. 3 clearly show that under the experimental conditions studied (C_o = 25 mg/L, pH 5, 25 °C, and 24 h agitation), the removal of mercury increases with increasing biosorbent dose. The removal of mercury increased from 60% at 0.5 g/L MSR dose to more than 90% at ~2 g/L MSR dose. The observed mercury uptake increase is attributed to the increased MSR surface area available for contact with the Hg(II), which leads to increased number of surface-active groups [25,26]. The mercury uptake remains practically the same, ~95%, at MSR dose >2 g/L. Furthermore, the mercury uptake does not appear to be linearly correlated with biosorbent dose, implying that mercury sorption onto MSR is not strictly a surface phenomenon.

3.3. Effect of contact time

The results from the kinetic experiments suggested that for the first 60 min the sorption of mercury onto MSR was rapid, (see Fig. 4). For the time period between 60 and 240 min the mercury uptake was considerably slower and reached a plateau for the time period 240–600 min. Subsequently, the uptake increased again and reached a second plateau at 1440 min. Double-plateau kinetic plots are commonly observed with porous sorbents [27]. However, based on the low BET values, MSR would not be considered as porous materials. Here the double plateau might be attributed to the swelling of the material, which takes place in a significant degree, as exhibited by dry impregnation experiments. MSR solids could increase up to 86 ± 0.6% their total volume due to water uptake. Most sorption processes take place by a multi-step mechanism, which may comprise of film diffusion, intraparticle diffusion, and physical or chemical sorption. In this study, various kinetic models were employed in order to assess the sorption kinetics of mercury onto MSR.

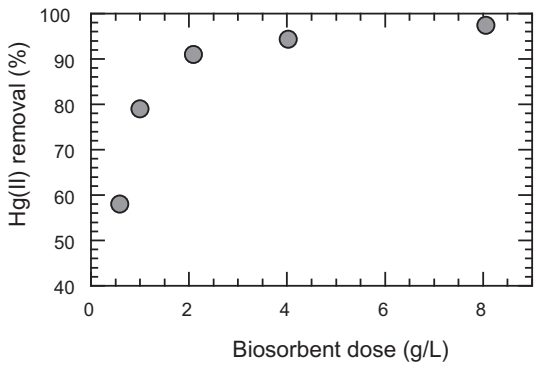

Fig. 3. Effect of biosorbent dose on Hg(II) removal after 24 h mixing. Here C_o = 25 mg Hg(II)/L, and pH 5.

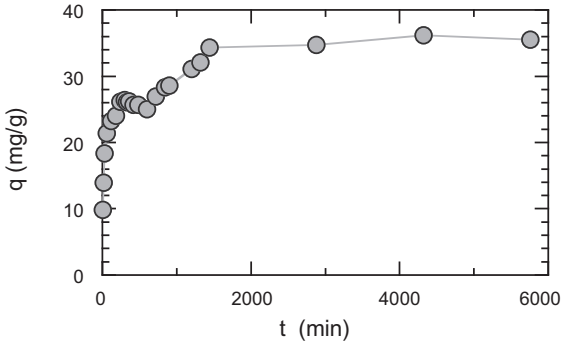

Fig. 4. Effect of contact time on Hg(II) uptake. Here C_o = 50 mg Hg(II)/L, and pH 5.

3.4. MSR–mercury interaction

FTIR analysis was performed on raw MSR and on MSR exposed to Hg(II) for 2 and 24 h in order to investigate the changes of the functional groups with time. The results are shown in Fig. 5. The bands between 3300 and 3000 cm^{-1} are attributed to —O—H bonds of carboxylic acids, and those between 3500 and 3300 cm^{-1} to —N—H bonds of amines, whereas the peaks at 1650 and 1058 cm^{-1} are attributed to —C=O and —C—O bonds of carboxylic acids, respectively. The peak at 1246 cm^{-1} suggests the presence of phosphonates. The spectra of the MSR exposed to Hg(II) reveal that all of the above mentioned groups are involved in the sorption process because the intensities of the various bands are significantly lower than those of the raw MSR. It is possible that carboxylic acids and amines contribute to mercury sorption for the time interval 2–24 h, because the intensity of the peaks of the other groups (i.e. phosphonates and hydroxyl groups) remain practically unchanged. Last, the band at 2400 cm^{-1} after sorption may be attributed to atmospheric CO_2 due to instrumentation related reasons and not sorption related ones.

3.5. Sorption isotherm

The experimental data were fitted to three isotherm models; linear, Freundlich (Fig. 6a), and Langmuir (Fig. 6b). The linear model does not fit the data well (R^2 = 0.19). The Langmuir model fits the data better (R^2 = 0.99) than the Freundlich model (R^2 = 0.88). The Langmuir model assumes that sorption occurs onto limited sites:

$$q_e = \frac{q_{\max} K_L C_e}{1 + (K_L C_e)} \quad (1)$$

where q_e (mg/g) is the equilibrium mercury mass per unit mass of biosorbent; $q_{\max}$ (mg/g) is the monolayer capacity of biosorbent;

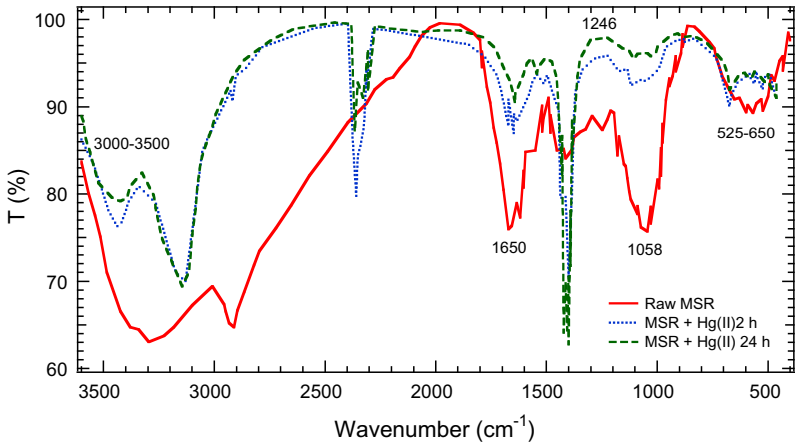

Fig. 5. FTIR spectrum of MSR at different contact times. Here C_o = 50 mg Hg(II)/L, and pH 5.

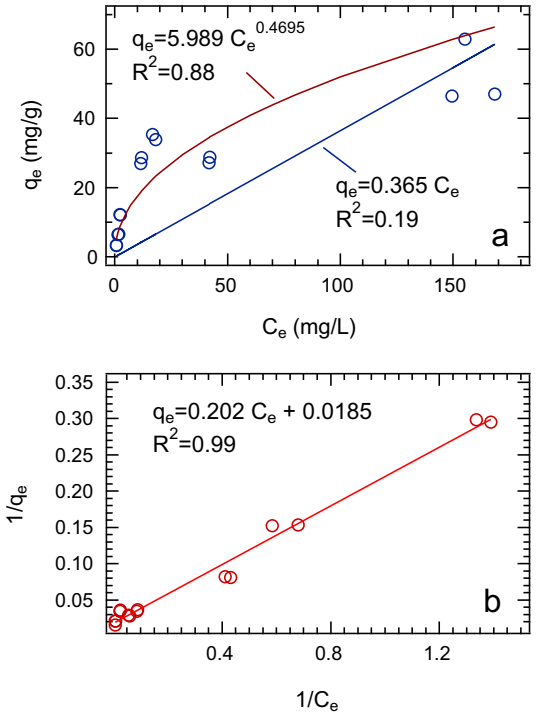

Fig. 6. Experimental data (symbols) of Hg(II) sorption onto MSR at pH = 5 and 24 h contact time fitted with (solid curves): (a) linear and Freundlich models, and (b) linearized form of the Langmuir model equation.

K_L (L/mg) is the Langmuir constant; and C_e is the equilibrium mercury concentration in the solution (mg/L).

Based on the data presented in the linearized form of the Langmuir equation (Fig. 6b):

$$\frac{1}{q_e} = \frac{1}{q_{max} K_L}\frac{1}{C_e} + \frac{1}{q_{max}} \quad (2)$$

q_{max} = 54 mg/g and K_L = 0.092 L/mg. The successful fit of the nonlinear isotherm suggests that sorption sites for this material are limited by the functional groups found on the sorbent surface.

Table 1 presents the calculated sorption capacity (q_e) of MSR tested in the present study and other biosorbents, which have been frequently used under similar conditions by other investigators, that have also provided the required isotherm data for proper isotherm constant comparison. It is obvious that MSR compare well with other materials and actually, demonstrate a sorption capacity towards the higher end of values found in the literature.

Table 1
Sorption capacity at pH 5 ± 0.5.

Biosorbent	q_e (mg/g)	Reference
C_o = 100 mg/L, solid to liquid concentration 2.5 g/L		
MSR	33.3	Present study
Green algae	13.3–30.3	[14]
Red algae	28.8–33.5	[14]
Brown algae	26.6–37.3	[14]
Sunflower seeds	11.7	[14]
Bracken fern	32.2	[14]
Bracken fern	42.0	[15]
Pine tree bark	34.3	[14]
Leaves of castor tree	28.4	[12]
Waste activated sludge	31.6	[37]
Ulva lactuca biomass	39.0	[38]
Macrocystis purifera	26.3	[39]
Undaria Pinnatifida	33.8	[39]
C_o = 200 mg/L, solid to liquid concentration 1 g/L		
MSR	50.4	Present study
Carica papaya	32.0	[13]

3.6. Kinetic modeling

3.6.1. Reaction-based models

The reaction-based models employed in this study, together with the fitted parameters are given in Table 2. The available kinetic equations were compared based on the correlation coefficient (R^2) obtained from the corresponding linear plot, and the residual sum of squares (RSS):

$$\mathrm{RSS} = \sum_{i=1}^{n} (q^{exp} - q^{calc})^2 \quad (12)$$

where q^{exp} and q^{calc} are the experimental and predicted by the model values of q (mg/g), respectively, n is the number of experimental values, and the subscript $i = 1 \ldots n$ indicates the appropriate sample.

It is worth noting that none of the above mentioned kinetic models predict a double plateau and therefore they are not suitable to describe the full length of time of the kinetic experiments. Nevertheless, they are able to describe kinetic experiments consisting of a single plateau and thus, give a general idea of the reaction the present kinetic experiment follows, at least at early stages. In the present study, the kinetic models employed and the calculations used refer to the first 600 min.

Table 2
Estimated parameters for the kinetic models employed.

Kinetic model	Equation		Linear equation		Reaction constants	Equilibrium Hg(II) sorption q_e (mg/g)	RSS	R^2
First-order	$q_t = q_e e^{-k_1 t}$	(3)	$\ln[q_t] = \ln[q_e] - k_1 t$	(8)	$k_1 = 10^{-4}$ min^{-1}	22	1524	0.35
Pseudo first-order	$\frac{dq}{dt} = k_{1p}(q_e - q)$	(4)	$\ln[q_e - q_t] = \ln[q_e] - k_{1p} t$	(9)	$k_1 = 10^{-3}$ min^{-1}	18	7517	0.85
Second-order	$q = \frac{q_e}{1+q_e k_2 t}$	(5)	$\frac{1}{q} = \frac{1}{q_e} + k_2 t$	(10)	$k_2 = 5 \times 10^{-6}$ g/mg min	21	2663	0.21
Pseudo second-order	$\frac{dq}{dt} = k_2(q_e - q_t)^2$	(6)	$\frac{t}{q} = \frac{1}{k_{2p} q_e^2} + \frac{1}{q_e} t$	(11)	$k_{2p} = 2 \times 10^{-4}$ g/mg min, $k_{2p} q_e^2 = 0.28$ mg/g min	36	534	0.99
Elovich	$q = \frac{1}{b}\ln[ab] + \frac{1}{b}\ln[t]$	(7)			$a = 14$ mg/g min $b = 0.27$ g/mg		43	0.95

Note: q_t (mg/g) and q_e (mg/g) are the quantity of mercury sorbed per mass unit of biosorbent at a given time t, and at equilibrium, respectively; k_1 (min^{-1}) is the first-order rate constant; k_{1p} (min^{-1}) is the pseudo-first-order rate constant; k_2 (g/mg min) is the second-order rate constant; k_{2p} (g mg/min) is the pseudo-second-order rate constant; a (mg/g min) is the initial sorption rate; b (g/mg) is related to the extent of surface coverage and activation energy for chemisorptions.

It is obvious that both the first-order model and the pseudo-first-order model yield a high RSS and low R^2 values. This leads to the conclusion that first-order models in general do not seem to be suitable to describe our experimental data at early times. The second-order model also yields a poor fit to our experimental data. However, the pseudo-second-order model describes the experimental results well, yielding a high correlation coefficient, a low normalized standard deviation, and the estimated value of the maximum sorption capacity approaches the experimental value. The pseudo-second-order model assumes that two reactions are occurring, the first one is fast and reaches equilibrium quickly, and the second is a slower reaction that continues for a long time period. The reactions can occur either in series or in parallel [28,29]. The Elovich model also matches the kinetic data well, indicating that chemisorption is strongly involved in the sorption process.

3.6.2. Diffusion based models

The sorption of a solute present in a solid-solution system is usually assumed to consist of four consecutive steps: external mass transfer of sorbate molecules across the boundary liquid film, binding of sorbate molecules on the active sites on the surface of the sorbent, intra-particle diffusion of sorbate molecules, and sorption of sorbate molecules on the active sites distributed within the sorbent particles. Generally, the steps involving binding are rapid and can be neglected when evaluating the rate-determining step of the sorption process [30].

To investigate the potential role of intra-particle diffusion on Hg(II) sorption, the Weber–Morris model was used [31]:

$$q = k_{id}\, t^{1/2} + C \tag{13}$$

where k_{id} is the intra-particle diffusion rate constant (mg/g min$^{1/2}$), and C is (mg/g) the y-intercept. Linearity of the plot of q versus $t^{1/2}$ denotes the presence of intra-particle diffusion. If $C = 0$, then intra-particle diffusion is the rate-controlling step, whereas if $C \neq 0$, intra-particle diffusion is not the rate-controlling step, but film diffusion plays an important role in the metal sorption process.

The Weber–Morris plot of the experimental data is shown in Fig. 7. Clearly, the plot consists of five linear parts. The first part (0–60 min) represents the external mass transfer, the second part (60–240 min) represents the intra-particle diffusion, and the third part (240–600 min) represents an apparent saturation where diffusion plays no role [30]. The fourth part in the plot (600–1440 min) may represent intra-particle diffusion, whereas the sorbate molecules are diffused further into the pores of the biomaterial till a final equilibrium is reached. This final equilibrium is represented by the fifth linear portion of the plot (1440–5760 min). The intra-particle diffusion rate constants for the second and fourth linear portions of the plot were estimated to be 0.58 ± 0.08 mg/g min$^{1/2}$ and 0.62 ± 0.05 mg/g min$^{1/2}$, respectively. These two rates are considered similar. Nonetheless, C was $\neq 0$ in both cases, namely 16 ± 3 and 10 ± 1 respectively, indicating that intra-particle diffusion was not the rate-controlling step, and that film diffusion significantly contributed to the sorption process [32].

In order to assess which process, external mass transfer or intra-particle diffusion, exerts greater influence on the rate of metal sorption, the Boyd film-diffusion model was employed. This model assumes that the main resistance to diffusion is the boundary layer surrounding the particle and is expressed as [33]:

$$F(t) = 1 - \left(\frac{6}{\pi^2}\right)\sum_{m=1}^{\infty}\left(\frac{1}{m^2}\right)e^{-m^2 Bt} \tag{14}$$

where $F(t)$ is the fraction of the solute absorbed at different times t:

$$F(t) = \frac{q}{q_e} \tag{15}$$

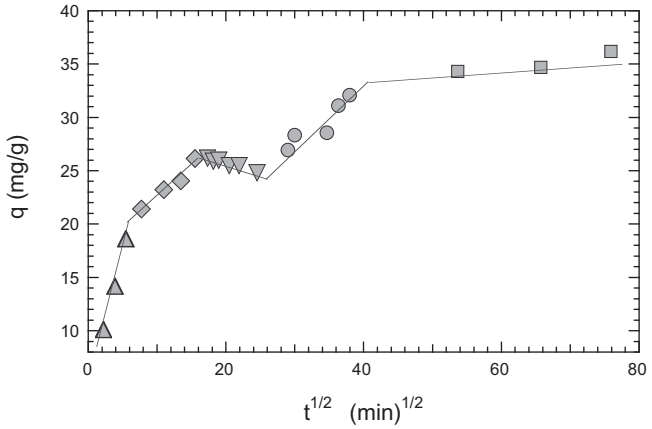

Fig. 7. Intraparticle diffusion of Hg(II) onto MSR for $C_o = 50$ mg Hg(II)/L and pH 5.

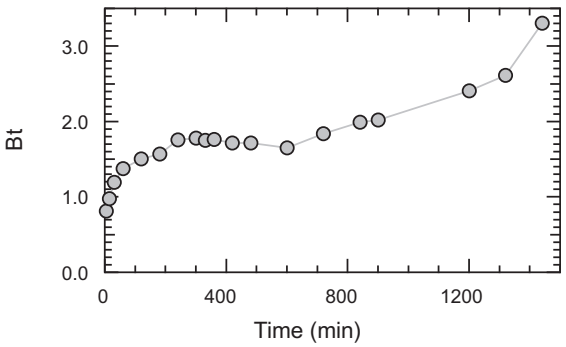

Fig. 8. Plot of Bt versus time (Boyd plot).

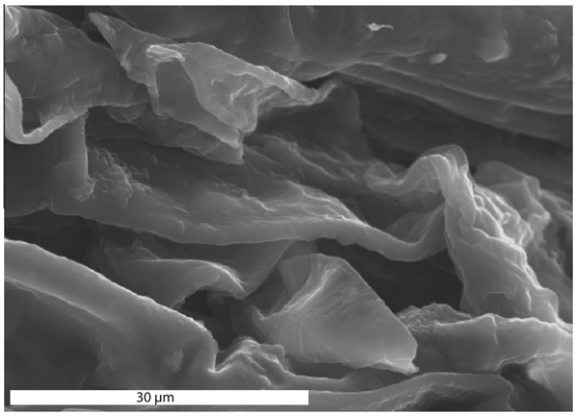

Fig. 9. SEM image of MSR after a 24-h contact time with C_o = 50 mg Hg(II)/L at pH 5.

and *Bt* is given by [34]:

$$Bt = 0.4977 - \ln[1 - F(t)] \quad (16)$$

The Boyd plot is obtained by plotting *Bt* versus *t* (see Fig. 8), showing multi-linearity over the time period studied, without passing through the origin (intercept = 0.7 ± 0.01), thus rendering quite difficult to predict whether external mass transfer or intra-particle diffusion is the rate controlling step. In conclusion, it seems that external mass transfer, film diffusion and intra-particle diffusion contribute to the sorption of mercury onto MSR, verifying that biosorption is a relatively complicated and multi-mechanism process.

The SEM analysis of the MSR after a 24 h contact with 50 mg Hg(II)/L revealed that mercury was adsorbed onto the entire surface of the MSR, and note that deposits of mercury were not observed (see Fig. 9).

Table 3
Desorption of Hg(II) from various sorbents.

Sorbent	Desorption medium	Contact time (min)	Desorption (%)	Reference
Malt spent rootlets	HCl 0.1–1 M	1440	50–54	Present study
Aminated chitosan beads	HCl 0.1 M	100[a]	65	[40]
Lichen biomass (*Xanthoparmelia conspersa*)	HCl 1 M		98	[35]
Castor tree leaves (*Ricinus communis* L.)	HCl 1–3 M HCl 4–6 M	30 30	60–84 98–99	[12]
Ulva lactuca biomass	H_2SO_4 0.3 N[b]		~100	[38]
Malt spent rootlets	HNO_3 0.1 M	1440	26	Present study
Aminated chitosan beads	HNO_3 0.1 M	100[a]	61	[40]
Malt spent rootlets	EDTA 0.1 M	1440	27	Present study
Aminated chitosan beads	EDTA 0.001–0.1 M	100[a]	48–95	[40]
Malt spent rootlets	NaCl 0.1–1 M	1440	39–44	Present study
Microalgae (*Chlamydomonas reinhardtii*)	NaCl 2 M	120[c]	>95	[23]
Fruit shell (*Terminalia catappa*)	KI (0.5–2%)	60	85–96	[41]

[a] Agitation rate 150 rpm.
[b] The regenerated biosorbent was reused for up to five adsorption–desorption cycles without loss of the biosorption capacity.
[c] At 200 rpm.

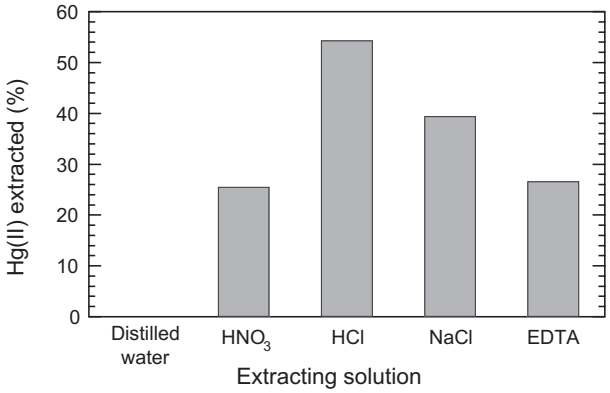

Fig. 10. Effect of extracting solutions (0.1 M) on Hg(II) desorption after 24 h mixing at initial q = 31.8 ± 2.4 mg Hg(II)/g MSR, solid to liquid ratio of 10 mg MSR/10 mL extracting solution, and 25 °C.

3.7. Mercury desorption

Different eluting agents with varying concentrations have been reported in the literature to facilitate desorption of mercury from various materials, i.e. HCl and HNO_3 with lichen biomass [35], HNO_3 with sewage sludge carbon [9], EDTA-disodium salt with microporous titanosilicate ETS-4 [36]. Desorption of Hg(II) from MSR was examined in order to investigate the feasibility of recovering Hg(II) using some common desorption agents. The effect of various leaching solutions on the desorption of Hg(II) from various sorbents found in the literature and in the present study is presented in Table 3.

The desorption results of four leaching solutions (0.1 M) and distilled water are presented in Fig. 10. The initial q for the experiments conducted was 32 ± 2 mg Hg(II)/g MSR. HCl resulted in the highest extraction percentage (54%) of the sorbed Hg(II). The increase of the concentration of HCl from 0.1 to 1 M did not significantly improve the mercury extraction efficiency. The increase of NaCl concentration from 0.1 to 0.2, 0.5, and 1 M resulted in slightly increased extraction capacity from 39% to 42%, 41%, and 44%, respectively. Note that raising the concentration of either NaCl or HCl up to 1 M did not affect the desorption capacity. Acid concentrations higher than 1 M might incur non desirable morphological alterations to the biomass, which renders it non re-usable in continuous sorption–desorption cycles.

4. Conclusions

Malt spent rootlets appear to be a promising biosorbent for the removal of mercury from aquatic systems. MSR exhibit satisfactory sorption capacity and fast kinetics. MSR are able to remove significant amounts of mercury even at strongly acidic conditions, a trait that might be useful for the treatment of mining effluents containing mercury. Kinetic and isotherm experiments revealed that biosorption is a complicated process with more than one mechanisms involved. This plethora of mechanisms is related to the sorbent's active groups. The removal of mercury increased from 60% to more than 90% with 0.5–2 g/L MSR, while it remained steady at 95% for MSR > 2 g/L. Preliminary desorption studies showed that mercury desorption from the MSR was most effective with 0.1 M HCl and 1 M NaCl, resulting in 54% and 44% extraction efficiencies, respectively.

References

[1] Q. Wang, D. Kim, D.D. Dionysiou, G. Sorial, D. Timberlake, Sources and remediation for mercury contamination in aquatic systems – a literature review, Environ. Pollut. 131 (2004) 323–336.
[2] EC, 2001. Decision No. 2455/2001/EC of 20 November 2001. Establishing the list of priority substances in the field of water policy and amending Directive 2000/60/EC. Official Journal of the European Communities, L 331, 15.12.2001, pp. 1–5.
[3] EC, 2008. Directive 2008/105/EC of the European Parliament and of the Council of 16 December 2008 on environmental quality standards in the field of water policy, amending and subsequently repealing Council Directives 82/176/EEC, 83/513/EEC, 84/156/EEC, 84/491/EEC, 86/280/EEC and amending Directive 2000/60/EC of the European Parliament and of the Council. Official Journal of the European Communities, L 348, 24.12.2008, pp. 84–97.
[4] S. Innanen, The ratio of anthropogenic to natural mercury release in Ontario: three emission scenarios, Sci. Total Environ. 213 (1998) 25–32.
[5] N. Pirrone, S. Cinnirella, X. Feng, R.B. Finkelman, H.R. Friedli, J. Leaner, R. Mason, A.B. Mukherjee, G.B. Stracher, D.G. Streets, K. Telmer, Global mercury emissions to the atmosphere from anthropogenic and natural sources, Atmos. Chem. Phys. 10 (2010) 5951–5964.
[6] B. Volesky, Sorption and Biosorption, SV Sorbex Inc., Montreal, 2003.
[7] J. Wang, C. Chen, Biosorbents for heavy metals removal and their future, Biotechnol. Adv. 27 (2009) 195–226.
[8] W.A. Ahmad, J. Jaapar, M.A.K.M. Zahari, Removal of heavy metals from wastewater, in: A. Pandey (Ed.), Concise Encyclopedia of Bioresource Technology, The Haworth Press Inc., New York, 2004, pp. 152–157.
[9] F.-S. Zhang, J.O. Nriagu, H. Itoh, Mercury removal from water using activated carbons derived from organic sewage sludge, Water Res. 39 (2005) 389–395.
[10] B.A.F. Mibeck, E.S. Olson, S.J. Miller, $HgCl_2$ sorption on lignite activated carbon: analysis of fixed-bed results, Fuel Process. Technol. 90 (2009) 1364–1371.
[11] E.-A. Kim, A.L. Seyfferth, S. Fendorf, R.G. Luthy, Immobilization of Hg(II) in water with polysulfide-rubber (PSR) polymer-coated activated carbon, Water Res. 45 (2011) 453–460.
[12] S.W. Al Rmalli, A.A. Dahmani, M.M. Abuein, A.A. Gleza, Biosorption of mercury from aqueous solutions by powdered leaves of castor tree (*Ricinus communis* L.), J. Hazard. Mater. 152 (2008) 955–959.
[13] S. Basha, Z.V.P. Murthy, B. Jha, Sorption of Hg(II) onto *Carica papaya*: experimental studies and design of batch sorber, Chem. Eng. J. 147 (2009) 226–234.
[14] L. Carro, R. Herrero, J.L. Barriada, M.E. Sastre de Vicente, Mercury removal: a physicochemical study of metal interaction with natural materials, J. Chem. Technol. Biotechnol. 84 (2009) 1688–1696.
[15] L. Carro, V. Anagnostopoulos, P. Lodeiro, J.L. Barriada, R. Herrero, M.E. Sastre de Vicente, A dynamic proof of mercury elimination from solution through a combined sorption–reduction process, Bioresource Technol. 101 (2010) 8969–8974.
[16] A.M. Deshicar, S.S. Bokade, S.S. Dara, Modified *hardwickia binata* bark for adsorption of mercury (II) from water, Water Res. 24 (1990) 1011–1016.
[17] Y. Goksungur, S. Uren, U. Guvenc, Biosorption of cadmium and lead ions by ethanol treated waste baker's yeast biomass, Bioresource Technol. 96 (2005) 103–109.
[18] Z.R. Holan, B. Volesky, Biosorption of lead and nickel by biomass of marine algae, Biotechnol. Bioengery 43 (1994) 1001–1009.
[19] W.R. Knocke, L.H. Hemphill, Mercury(II) sorption by waste rubber, Water Res. 15 (1981) 275–282.
[20] J.O. Leckie, R.O. James, Control Mechanisms for Trace Metals in Natural Waters, Ann Arbor Science Publishers, New York, 1974.
[21] J. Karthikeyan, M. Chaudhuri, Enhancement of mercury(II) sorption from water by coal through chemical pretreatment, Water Res. 20 (1986) 449–452.
[22] L. Svecova, M. Spanelova, M. Kubal, E. Guibal, Cadmium, lead and mercury biosorption on waste fungal biomass issued from fermentation industry. I. Equilibrium studies, Sep. Purif. Technol. 52 (2006) 142–153.
[23] G. Bayramoğlu, I. Tuzun, G. Celik, M. Yilmaz, M.Y. Arica, Biosorption of mercury(II), cadmium(II) and lead(II) ions from aqueous system by microalgae Chlamydomonas reinhardtii immobilized in alginate beads, Int. J. Miner. Process. 81 (2006) 35–43.
[24] R. Laus, R. Geremias, H.L. Vasconcelos, M.C. Laranjeira, V.T. Favere, Reduction of acidity and removal of metal ions from coal mining effluents using chitosan microspheres, J. Hazard. Mater. 149 (2007) 471–474.
[25] T. Akar, Z. Kaynak, S. Ulusoy, D. Yuvaci, G. Ozsari, S.T. Akar, Enhanced biosorption of nickel(II) ions by silica-gel-immobilized waste biomass: biosorption characteristics in batch and dynamic flow mode, J. Hazard. Mater. 163 (2009) 1134–1141.
[26] W. Shao, L. Chen, L. Lü, F. Luo, Removal of lead (II) from aqueous solution by a new biosorption material by immobilizing Cyanex272 in cornstalks, Desalination 265 (2011) 177–183.
[27] I. Devotta, R.A. Mashelkar, Competitive diffusion–adsorption of polymers of differing chain lengths on solid surfaces, Chem. Eng. Sci. 51 (1996) 561–569.
[28] M.L. Brusseau, P.S.C. Rao, Sorption non-ideality during organic contaminant transport in porous media, Crit. Rev. Environ. Control. 19 (1984) 33–39.
[29] Y. Khambhaty, K. Mody, S. Basha, B. Jha, Kinetics, equilibrium and thermodynamic studies on biosorption of hexavalent chromium by dead fungal biomass of marine *Aspergillus niger*, Chem. Eng. J. 145 (2009) 489–495.
[30] D. Kumar, J.P. Gaur, Chemical reaction- and particle diffusion-based kinetic modeling of metal biosorption by a *Phormidium sp.*-dominated cyanobacterial mat, Bioresource. Technol. 102 (2011) 633–640.
[31] W.J. Weber, J.C. Morris, Kinetics of adsorption on carbon from solution, J. San. Eng. Div. 89 (1963) 31–60.
[32] Y.S. Al-Degs, M.I. El-Barghouthi, A.A. Issa, M.A. Khraisheh, G.M. Walker, Sorption of Zn(II), Pb(II), and Co(II) using natural sorbents: Equilibrium and kinetic studies, Water Res. 40 (2006) 2645–2658.
[33] G.E. Boyd, A.W. Adamson, L.S. Myers Jr., The exchange adsorption of ions from aqueous solutions by organic zeolites. II. Kinetics, J. Am. Chem. Soc. 69 (1947) 2836–2848.
[34] D. Reichenberg, Properties of ion exchange resins in relation to their structure. III. Kinetics of exchange, J. Am. Chem. Soc. 75 (1952) 589–598.
[35] M. Tuzen, A. Sari, D. Mendil, M. Soylak, Biosorptive removal of mercury(II) from aqueous solution using lichen (*Xanthoparmelia conspersa*) biomass: kinetic and equilibrium studies, J. Hazard. Mater. 169 (2009) 263–270.
[36] C.B. Lopes, E. Pereira, Z. Lin, P. Pato, M. Otero, C.M. Silva, J. Rocha, A.C. Duarte, Fixed-bed removal of Hg2+ from contaminated water by microporous titanosilicate ETS-4: experimental and theoretical breakthrough curves, Microporous Mesoporous Mater. 145 (2011) 32–40.
[37] M. Kılıc, M.E. Keskin, S. Mazlum, N. Mazlum, Effect of conditioning for Pb(II) and Hg(II) biosorption on waste activated sludge, Chem. Eng. Process. 47 (2008) 31–40.
[38] Y. Zeroual, A. Moutaouakkil, F.Z. Dzairi, M. Talbi, P.U. Chung, K. Lee, M. Blaghen, Biosorption of mercury from aqueous solution by *Ulva lactuca* biomass, Bioresource Technol. 90 (2003) 349–351.
[39] J. Plaza, M. Viera, E. Donati, E. Guibal, Biosorption of mercury by Macrocystis pyrifera and Undaria pinnatifida: influence of zinc, cadmium and nickel, J. Environ. Sci. 23 (2011) 1778–1786.
[40] C. Jeon, K.H. Park, Adsorption and desorption characteristics of mercury (II) ions using aminated chitosan bead, Water Res. 39 (2005) 3938–3944.
[41] B.S. Inbaraj, N. Sulochama, Mercury adsorption on a carbon sorbent derived from fruit shell of *Terminalia catappa*, J. Hazard. Mater. B133 (2006) 283–290.